Interacting electrons in graphene nanoribbons in the lowest Landau level

Artsem Shylau and Igor Zozoulenko

Original Publication:

Artsem Shylau and Igor Zozoulenko, Interacting electrons in graphene nanoribbons in the lowest Landau level, 2011, Physical Review B. Condensed Matter and Materials Physics, (84), 7, 075407.
http://dx.doi.org/10.1103/PhysRevB.84.075407

Interacting electrons in graphene nanoribbons in the lowest Landau level

A. A. Shylau* and I. V. Zozoulenko†
Solid State Electronics, ITN, Linköping University, 601 74 Norrköping, Sweden
(Received 27 April 2011; published 2 August 2011)

We study the effect of electron-electron interaction and spin on electronic and transport properties of gated graphene nanoribbons (GNRs) in a perpendicular magnetic field in the regime of the lowest Landau level (LL). The electron-electron interaction is taken into account using the Hartree and Hubbard approximations, and the conductance of GNRs is calculated on the basis of the recursive Greens function technique within the Landauer formalism. We demonstrate that, in comparison to the one-electron picture, electron-electron interaction leads to the drastic changes in the dispersion relation and structure of propagating states in the regime of the lowest LL showing a formation of the compressible strip and opening of additional conductive channels in the middle of the ribbon. We show that the latter are very sensitive to disorder and get scattered even if the concentration of disorder is moderate. In contrast, the edge states transport is very robust and cannot be suppressed even in the presence of a strong spin-flipping.

DOI: 10.1103/PhysRevB.84.075407 PACS number(s): 72.80.Vp, 73.22.Pr, 73.43.Cd, 73.43.Qt

I. INTRODUCTION

Due to Dirac spectrum graphene possesses a number of unique electronic and transport properties.[1] In a magnetic field B perpendicular to a graphene layer the spectrum is modified into a series of Landau levels (LL) with the energies $E = \pm\hbar\omega_c\sqrt{|N|}$, where the cyclotron frequency $\omega_c = v_F\sqrt{2eB/\hbar}$, $v_F \approx 10^8$ cm/s is the Fermi velocity and $N = 0, \pm 1, \pm 2, \ldots$ (Ref. 2). One of the interesting features of this spectrum is a presence of zeroth LL with $E = 0$, which is equally shared between electrons and holes. In contrast to conventional two-dimensional electron gas systems the position of this level does not depend on a value of the magnetic field. An experimental manifestation of these unusual series is the anomalous quantum Hall effect with the Hall conductivity given by $\sigma_{xy} = \frac{4e^2}{h}(N + 1/2)$, where the factor of 4 comes from the spin and valley degeneracy.[3,4] In a strong magnetic field the four-fold degeneracy of the lowest (i.e., zeroth) LL is lifted leading to the insulating behavior characterized by the presence of additional plateaux in the Hall conductivity σ_{xy} accompanied by the increase of the longitudinal resistivity ρ_{xx} (Refs. 5–7). The large energy gaps identified experimentally suggests that electron-electron interactions along with the Zeeman spin-splitting play an important role in understanding of this phenomena.

Most of the experiments reported so far are performed in the four-terminal geometry which allows a direct measurement of the components of the resistivity and conductivity tensors.[5–8] However, in some cases the only possible experimental setup is the two-terminal measurements, even though the results obtained in this geometry are not as straightforward to interpret as the four-terminal ones.[9] A difference between the longitudinal and the Hall resistances is not clearly defined in such the measurements. The unexpected consequence of analysis of the two-terminal geometry is that a measured two-terminal resistance between the right and left contacts, R_{2t}, corresponds, in the four-terminal setup, to the Hall resistance R_H rather than to the longitudinal one R_L. This stems from the fact that the voltage drop between the sample edges, V, equals to the difference of the chemical potentials in the contacts $eV = \mu_R - \mu_L$ (Refs. 10 and 11).

An explanation of the quantum Hall effect is often based on the picture of edge states. In a strong enough magnetic field the right and left propagating states are localized at different edges of the system due to the Lorentz force. It leads to exponentially small overlap between counterpropagating states which, in turn, greatly suppresses a possibility of backscattering and is eventually manifested by developing pronounced plateaux in the conductance. In graphene another transport regime can be realized.[12] Coupling of spin to magnetic field due to the Zeeman effect leads to a splitting of the lowest LLs into two sublevels. For the neutral graphene the chemical potential coincides with the zero energy and lies in the center of the spin gap, see Fig. 1 and Fig. 2(d) below. At a given Fermi energy there are two forward propagating states of opposite spins located near different edges. The most prominent feature of this transport regime is that forward and backward propagating states of the different spins are not spatially separated. If a scattering event leads to a spin flipping, the overlap between the counterpropagating states of different spins might be sufficient to cause the backscattering. This backscattering of the spin-polarized states is used for an explanation of the nonzero behavior of ρ_{xx} near the Dirac point.[13]

It should be stressed that the structure of edge states derived within a one-electron approximation and shown in Fig. 2(d) corresponds to the case of neutral graphene when the electron density is zero. It is often used for understanding and explanation of a variety of experiments on magnetotransport.[14] The conditions for existence of the edge states in graphene nanoribbons (GNRs) was discussed in details in Ref. 15. Also, self-consistent Hartee-Fock calculations were performed for GNR in magnetic field.[16] It was shown than the favored ground states in the neutral graphene are charge- or spin-density waves. Neither of these orderings support the edge states. However, in experiments one usually needs to tune a charge concentration by means of the gate voltage. It was shown before that electron-electron interaction between induced charges can dramatically change the energy dispersion and the structure of propagating states.[17–19] The magnetosubband structure and the character of propagating states in the lowest LL for the case of nonzero induced charge density remain largely unexplored and represent the main focus of

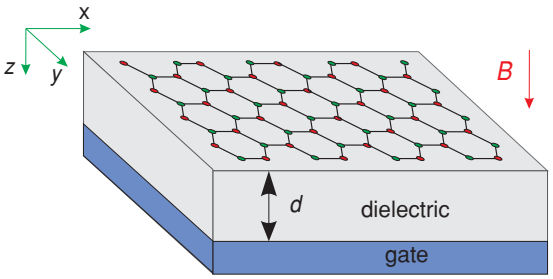

FIG. 1. (Color online) A schematic layout illustrating a system consisting of a graphene nanoribbon of the width $w = 20$ nm which is located on an insulating substrate at the distance $d = 300$ nm apart from a metallic back gate. The whole system is subjected to a perpendicular magnetic field $B = 150$ T.

the present study. We investigate the effect of the electron-electron interaction, spin, and global gate electrostatics on magnetotransport properties of GNR in the vicinity of the charge neutrality point. Based on the calculated self-consistent magnetosubband structure we compute and analyze the two-terminal conductance of realistic GNRs focusing on the effect of disorder, surface warping, and spin flipping on the robustness of the edge state transmission.

II. MODEL

We consider a system consisting of a GNR of the width $w = 20$ nm and the length $l = 85$ nm, located on an insulating substrate ($\epsilon_r = 3.9$) and connected to ideal graphene leads of the same width, see Fig. 1. A metallic back gate is used to tune the Fermi energy and the charge concentration in the GNR. The whole system is subjected to a uniform magnetic field, $B = 150$ T, perpendicular to the graphene plane. Such the high value of the magnetic field allows us to use relatively narrow GNR (to reduce computational time) and choose the ratio $w/l_B \approx 9.5$ in accordance with typical experiments (with $l_B = \sqrt{\hbar/eB}$ being the magnetic length). To model magnetotrasport in a GNR we use the tight-binding Hubbard Hamiltonian in the mean-field approximation $H = H_\uparrow + H_\downarrow$ which is shown to describe carbon electron systems in good agreement with first-principles calculations,[20]

$$H_\sigma = -\sum_{\mathbf{r},\Delta} t_{\mathbf{r},\mathbf{r}+\Delta} a^+_{\mathbf{r}\sigma} a_{\mathbf{r}+\Delta,\sigma} + g\mu_b B\sigma \sum_{\mathbf{r}} a^+_{\mathbf{r}\sigma} a_{\mathbf{r}\sigma} + \sum_{\mathbf{r}} V_H(\mathbf{r}) a^+_{\mathbf{r}\sigma} a_{\mathbf{r}\sigma} + U \sum_{\mathbf{r}} \left(\langle n_{\mathbf{r}\sigma'} \rangle - \frac{1}{2} \right) a^+_{\mathbf{r}\sigma} a_{\mathbf{r}\sigma}, \quad (1)$$

where σ, σ' describe two opposite spin states $\uparrow, \downarrow$; the summation runs over all sites of the graphene lattice, Δ includes the nearest neighbors only, $t_{\mathbf{r},\mathbf{r}+\Delta} = t_0 \exp(i 2\pi \phi_{\mathbf{r},\mathbf{r}+\Delta}/\phi_0)$ with

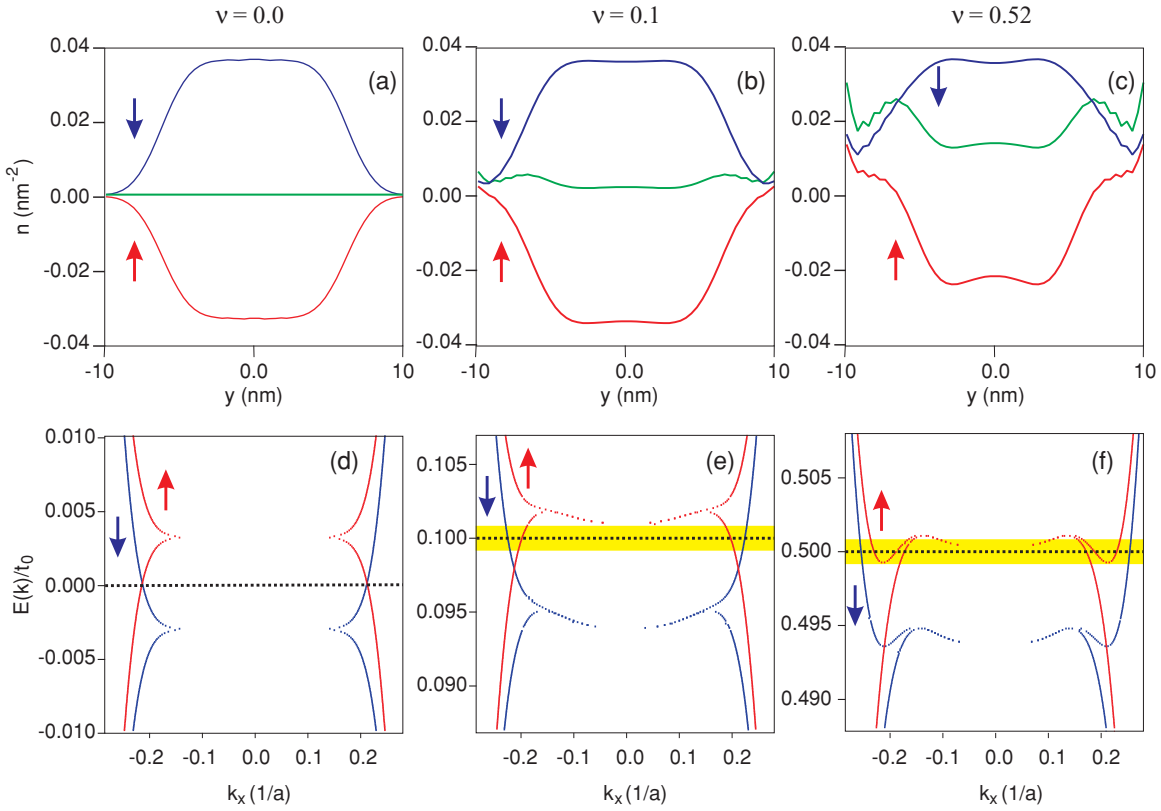

FIG. 2. (Color online) (a)–(c) Charge density distributions, and (d)–(f) band structure of a graphene nanoribbon in a perpendicular magnetic field $B = 150$ T. (a, d) one-electron approximation, $eV_g/t_0 = 0$; (b, e) self-consistent calculations for $eV_g/t_0 = 0.1$ and (c), (f) $eV_g/t_0 = 0.5$. Red and blue curves marked by $\uparrow$ and $\downarrow$ correspond to the charge densities of spin-up and spin-down electrons, respectively, $n_\uparrow(y)$,$n_\downarrow(y)$. Charge densities are averaged over three successive sites. Green curves correspond to the total density distribution $n(y) = n_\uparrow(y) + n_\downarrow(y)$. Dashed lines define the Fermi energy position. Yellow fields correspond to the energy interval $[-2\pi k_B T, 2\pi k_B T]$; temperature $T = 4.2$ K.

$t_0 = 2.77$ eV, $\phi_0 = h/e$ being the magnetic flux quantum which is calculated using the Pierel's substitution

$$\phi_{\mathbf{r},\mathbf{r}+\Delta} = \int_{\mathbf{r}}^{\mathbf{r}+\Delta} \mathbf{A}\cdot d\mathbf{l}, \tag{2}$$

with $\mathbf{A}$ being the vector potential. [In our calculations we use the Landau gauge, $\mathbf{A} = (-By,0)$]. The first term in the Hamiltonian (1) describes hopping of electrons through the graphene lattice. The second term describes the spin-splitting in the magnetic field B due to the Zeeman effect. Both these terms correspond to the non-interacting part of the Hamiltonian. The interaction between electrons of the opposite spins is described by the Hubbard term with $U = 1.33t_0$ (Refs. 16 and 21), and $V(\mathbf{r})$ is a Hartree term describing the long-range Coulomb interaction between induced charges in the GNR,[18,22]

$$V_H(\mathbf{r}) = \frac{e^2}{4\pi\varepsilon_0\varepsilon_r}\sum_{\mathbf{r}'\neq\mathbf{r}} n(\mathbf{r}')\left(\frac{1}{|\mathbf{r}-\mathbf{r}'|} - \frac{1}{\sqrt{|\mathbf{r}-\mathbf{r}'|^2+4d^2}}\right), \tag{3}$$

where d is the distance between the GNR and the gate, and the second term describes a contribution from the mirror charges. To calculate the electron number at site $\mathbf{r}$, Eq. (1) is solved using the recursive Green's function technique[23]

$$\langle n_{\mathbf{r}\sigma}\rangle = -\frac{1}{\pi}\int_{-\infty}^{\infty} \Im[G_\sigma(\mathbf{r},\mathbf{r},E)] f_{\mathrm{FD}}(E,E_F)dE, \tag{4}$$

where $G_\sigma(\mathbf{r},\mathbf{r},E)$ is the Green function in the real space representation of an electron of the spin σ residing on the site $\mathbf{r}$ and $E_F = eV_g$ is the Fermi energy which position is adjusted by the gate voltage. Equations (1)–(4) are solved self-consistently to compute the band structure, the charge density and the potential distribution. For a given potential distribution we compute the conductance using the Landauer formula

$$G(E_F,B) = G_0\int T(E,B)\left[-\frac{\partial f_{\mathrm{FD}}(E-E_F)}{\partial E}\right]dE, \tag{5}$$

where $T(E,B)$ is a total transmission coefficient, $G_0 = e^2/h$ is the conductance quantum, and f_{FD} is the Fermi-Dirac distribution.

All the results presented in this study correspond to the case of armchair nanoribbons. In the absence of magnetic field the most significant differences between nanoribbons with different edge termination are the presence of a zero-energy edge state in zigzag GNRs and the existence of semiconducting states in armchair GNRs. In a high magnetic field the difference between nanoribbons of different edge terminations practically diminishes as both zigzag and armchair GNRs acquire similar features related to the formation of the Landau levels. Therefore all the conclusions presented in the paper are generic to GNRs in a high magnetic field regardless of a type of the edge termination (armchair or zigzag).

III. RESULTS AND DISCUSSION

Figures 2(a)–2(c) show the charge density distribution and Figs. 2(d)–2(f) the magnetosubband structure of a GNR for several gate voltages, $eV_g/t_0 = 0$, 0.1, and 0.5, respectively, in the regime of the lowest LL, $|\nu| < 1$ ($\nu = nh/eB$ being the filling factor and n is the average charge concentration). An application of the gate voltage induces extra charges in the system, Figs. 2(b) and 2(c), which leads to an asymmetry between the electron and hole branches in the energy spectrum, see Figs. 2(e) and 2(f). For small gate voltages, see Fig. 2(e), the lowest unoccupied spin-up branch deforms and gets pinned to the Fermi energy. As a result, a region with compressible densities is formed in the center of the ribbon. We define the compressible strip as a region where the dispersion lies within the energy window $|E - E_F| \lesssim 2k_BT$ (Ref. 19). The compressible strips form because in the above energy window the states are partially filled (i.e., $0 \leqslant f_{\mathrm{FD}} \leqslant 1$) and hence the system has a metallic character. The formation of compressible strips in graphene has been recently discussed in Refs. 17 and 19. Further increase of the gate voltage leads to increase of the total electron density, which, in turn, causes even stronger pinning of the lowest LL to the Fermi energy such that the compressible strip gets extended almost over the entire ribbon, see Fig. 2(f). Figures 2(a)–2(c) show a density distribution for spin-up and spin-down electrons, $n_\uparrow(y)$,$n_\downarrow(y)$ and the total density distribution, $n(y) = n_\uparrow(y) + n_\downarrow(y)$. Due to the strong Zeeman splitting the electron branch is predominantly spin-up polarized, whereas the hole branch is spin-down polarized. The total charge distribution shows a density enhancement toward the ribbon's edges. This feature is related to the effect of the electrostatic Coulomb repulsion in a structure with a hard-wall confinement and was discussed (for the spinless case) in Refs. 17 and 18.

Compressible strips in GNRs are characterized by the existence of counterpropagating states at the same edge.[19] This can play an important role in understanding of the magnetotransport of interacting electrons in the vicinity of the Dirac point. In the one-electron picture the number of propagating states in the region $-1 < \nu < 1$ always equals to two with electrons of different spins propagating near different boundaries, see Fig. 2(d). [Note that a number of propagating states at a given energy is given by a number of intersections of the line $E = E_F$ with the dispersion bands $E = E(k)$, and the direction of the propagation is determined by a sign of $\partial E/\partial k_x$.] The backscattering is probable only in events accompanied by a spin-flipping since the counterpropagating states with the same spin are located at the different edges. However, in graphene a spin-relaxation length is rather large and can reach several micrometers,[24] therefore backscattering is expected to be rather unimportant. However, the situation is different when electron-electron interaction is taken into account. In this case there are a number of additional transport channels at the Fermi energy where electrons of the same spin propagate in the opposite directions at the same boundary, see Fig. 2(f). In this case no spin-flipping is apparently needed for the backscattering and the latter can be caused by impurity scattering of electrons of the same spin. To summarize, our self-consistent calculations demonstrate that, in comparison to the one-electron picture, electron-electron interaction leads to the drastic changes in the dispersion relation and structure of propagating states in the regime of the lowest LL such as a formation of the compressible strip and opening of additional conductive channels in the middle of the ribbon.

We proceed to the discussion of the conductance of GNRs in the regime of the lowest LL taking into account the electron

interaction and spin effects. We will study the effect of different types of disorder on GNR's conductance, focusing on the robustness of, respectively, edge and bulk state transmissions. Let us start with the case of an ideal GNR (i.e., without any disorder) whose conductance is shown in Fig. 3 as a red (solid) curve. In the range $0 < \nu \lesssim 0.3$ there are only two states in the energy interval $4\pi k_B T$ and the transport is determined by the edge states only, see Fig. 2(e) (note that in this range of ν the states in the compressible regions practically do not contribute to the conductance). As a result, the conductance of the ideal ribbon equals to $2G_0$. A further increase of the filling factor leads to the enhancement of the conductance due to the additional states forming the compressible strip, see Fig. 2(f). The conductance of the ideal ribbon is therefore not quantized and develops a bump-like structure with the increase of the filling factor above $\nu \gtrsim 0.3$. The suppression of conductance quantization in an ideal GNR in a perpendicular magnetic field for $\nu > 1$ was discussed in detail in Ref. 19.

Let us now study the effect of impurities on the conductance, see Fig. 3(a). Recent two-terminal measurements showed that the quantized conductance plateaux are not observed even in high magnetic field.[25–27] In particular, this behavior is attributed to the effect of impurities which can crosslink the chiral currents flowing at opposite edges.[25] We utilize the model of short-range impurities which are uniformly distributed over the GNR. They are modeled by adding to the self-consistent potential a term which is randomly chosen in the energy interval $[-\delta,\delta]$, where $\delta = 4t_0$ is an impurity strength. The concentration of impurities is chosen in the range (0.01–0.1) nm^{-2}. As expected, the states forming the compressible strip are the most sensitive to disorder. They propagate in the center of the ribbon and have a significant spatial extension in the transverse direction. When the concentration of impurities is moderate (green dotted and blue solid lines), the conductance decreases but remains larger than $2G_0$ since there are at least two edge states which transmit the current. The edge states are very robust and can be suppressed only if the impurity concentration greatly exceeds typical experimental values (green dashed line).

Another source of disorder can arise from a surface warping which is an inherent property of graphene.[28] Even though the magnetic field is uniform, a normal to the surface component of the magnetic field fluctuates due to the corrugated geometry of graphene. It results in a spatial-dependent hopping integrals. It has been shown that these spatial correlations can affect the quantum Hall (QH) transition at $E = 0$ leading to anomalously abrupt behavior[29] or result in a field-driven topological transition from the QH-metal state to the QH-insulator state in the vicinity of $\nu \simeq 0$ (Ref. 30). To take this effect into account we first generate a corrugated surface [see inset in Fig. 3(b)] using a method described in Refs. 31 and 32. Then graphene lattice is projected on the surface and a hopping integrals between two adjacent carbon atoms are calculated by integration of the vector potential along a line linking these atoms according to Eq. (2). We find that the conductance of the warped GNR is practically the same as that one of the ideal ribbon, see Fig. 3(b). We therefore conclude that for realistic nanoribbons the spatial modulation of the magnetic field due to the warping has a negligible effect on the conductance.

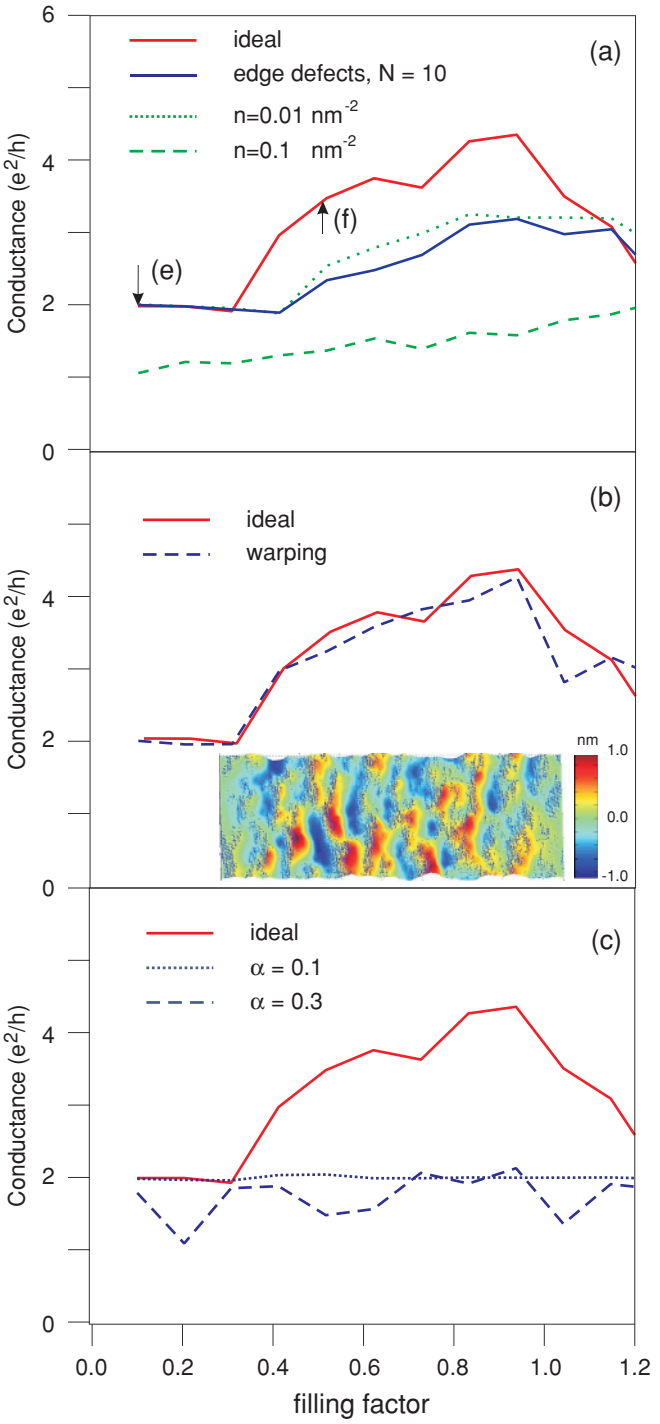

FIG. 3. (Color online) Conductance of the GNR as a function of the filling factor ν calculated in the presence of different types of disorder: (a) short-range impurities with strength $\delta = 4t_0$, (b) fluctuation of the normal to the surface component of the magnetic field due to the warping; (c) spin-flip effect. The red (solid) line on all plots corresponds to an ideal ribbon (i.e., without disorder). The arrows (e) and (f) indicate the filling factors for which the corresponding band structures are plotted in Figs. 2(e) and 2(f), respectively. The inset in (b) illustrates the landscape of a corrugated GNR. A typical wavelength of the ripples is about 8 nm, while the height fluctuates within 1 nm. $T = 4.2$ K.

Finally we investigate the effect of spin-flipping on the magnetotransport of GNRs. It is modeled by introducing in the Hamiltonian an additional term $H_{sf} = \alpha \sum_{\mathbf{r}} (a^+_{\mathbf{r}\uparrow} a_{\mathbf{r}\downarrow} + a^+_{\mathbf{r}\downarrow} a_{\mathbf{r}\uparrow})$, where α describes the local spin-flip rate. This term will in generally admix the counterpropagating states of different spins leading to backscattering. In our calculations the value of α is varied in the range $(0.0–0.3)t_0$ (Ref. 33). The conductance of GNRs in the presence of spin-flipping is shown in Fig. 3(c). When $\alpha = 0.1t_0$ (dotted line) the states constituting the compressible strips get scattered and the total conductance is only due to the edge states. As α increased up to $0.3t_0$ (dashed line) the conductance decreases below the value of $2G_0$ due to stronger scattering but still remains mostly dominated by the edge states. Backscattering of spin-polarized states due to spin-flipping was suggested as the way to manipulate spin currents.[12] As it was mentioned in the Introduction, this backscattering was also used to explain the nonzero behavior of ρ_{xx} near the Dirac point.[13] However, our results show that even in the case of strong admixture of counterpropagating states, the edge state transmission remains practically unaffected.

IV. CONCLUSION

The magnetotransport properties of GNRs in the regime of the lowest LL was studied taking into account electron interaction, gate electrostatic and spin effects. When the gate voltage is applied extra charges are induced in the ribbon leading to an asymmetry between the electron and hole branches in the energy spectrum. The lowest LL gets pinned to the Fermi energy and a compressible strip is formed in the middle of the GNR. There are two types of current carrying states in the lowest LL, the conventional edge states and the bulk states in the middle of the ribbon constituting the compressible strip. The latter are very sensitive to disorder and get scattered even if the concentration of disorder is moderate. In contrast, the edge states are very robust and cannot be suppressed even in the presence of a strong spin flipping.

ACKNOWLEDGMENT

We acknowledge support of the Swedish Research Council (VR).

*artsem.shylau@itn.liu.se
†igor.zozoulenko@itn.liu.se

[1] A. H. Castro Neto, F. Guinea, N. M. R. Peres, K. S. Novoselov, and A. K. Geim, Rev. Mod. Phys. **81**, 109 (2009).
[2] V. P. Gusynin and S. G. Sharapov, Phys. Rev. B **71**, 125124 (2005).
[3] K. S. Novoselov, A. K. Geim, S. V. Morozov, D. Jiang, M. I. Katsnelson, I. V. Grigorieva, S. V. Dubonos, and A. A. Firsov, Nature (London) **438**, 197 (2005).
[4] Y. Zhang, Y.-W. Tan, H. L. Stormer, and P. Kim, Nature (London) **438**, 201 (2005).
[5] J. G. Checkelsky, L. Li, and N. P. Ong, Phys. Rev. Lett. **100**, 206801 (2008).
[6] L. Zhang, J. Camacho, H. Cao, Y. P. Chen, M. Khodas, D. E. Kharzeev, A. M. Tsvelik, T. Valla, and I. A. Zaliznyak, Phys. Rev. B **80**, 241412(R) (2009).
[7] L. Zhang, Y. Zhang, M. Khodas, T. Valla, and I. A. Zaliznyak, Phys. Rev. Lett. **105**, 046804 (2010).
[8] A. J. M. Giesbers, U. Zeitler, M. I. Katsnelson, L. A. Ponomarenko, T. M. Mohiuddin, and J. C. Maan, Phys. Rev. Lett. **99**, 206803 (2007).
[9] J. R. Williams, D. A. Abanin, L. DiCarlo, L. S. Levitov, and C. M. Marcus, Phys. Rev. B **80**, 045408 (2009).
[10] T. Kramer, V. Krueckl, E. J. Heller, and R. E. Parrott, Phys. Rev. B **81**, 205306 (2010).
[11] Mark O. Goerbig, e-print arXiv:0909.1998v2.
[12] D. A. Abanin, P. A. Lee, and L. S. Levitov, Phys. Rev. Lett. **96**, 176803 (2006).
[13] D. A. Abanin, K. S. Novoselov, U. Zeitler, P. A. Lee, A. K. Geim, and L. S. Levitov, Phys. Rev. Lett. **98**, 196806 (2007).
[14] J. G. Checkelsky, L. Li, and N. P. Ong, Phys. Rev. B **79**, 115434 (2009).
[15] V. P. Gusynin, V. A. Miransky, S. G. Sharapov, and I. A. Shovkovy, Phys. Rev. B **77**, 205409 (2008).
[16] J. Jung and A. H. MacDonald, Phys. Rev. B **80**, 235417 (2009).
[17] P. G. Silvestrov and K. B. Efetov, Phys. Rev. B **77**, 155436 (2008).
[18] A. A. Shylau, J. W. Klos, and I. V. Zozoulenko, Phys. Rev. B **80**, 205402 (2009).
[19] A. A. Shylau, I. V. Zozoulenko, H. Xu, and T. Heinzel, Phys. Rev. B **82**, 121410(R) (2010).
[20] J. Fernández-Rossier and J. J. Palacios, Phys. Rev. Lett. **99**, 177204 (2007).
[21] O. V. Yazyev, Phys. Rev. Lett. **101**, 037203 (2008).
[22] J. Fernández-Rossier, J. J. Palacios, and L. Brey, Phys. Rev. B **75**, 205441 (2007).
[23] H. Xu, T. Heinzel, M. Evaldsson, and I. V. Zozoulenko, Phys. Rev. B **77**, 245401 (2008).
[24] N. Tombros, C. Jozsa, M. Popinciuc, H. T. Jonkman, and B. J. van Wees, Nature (London) **448**, 571 (2007).
[25] R. Rebeiro, J.-M. Poumirol, A. Cresti, W. Escoffier, M. Goiran, J.-M. Broto, S. Roche, and B. Raquet, e-print arXiv:1102.3300v1.
[26] J. B. Oostinga, B. Sacepe, M. F. Craciun, and A. F. Morpurgo, Phys. Rev. B **81**, 193408 (2010).
[27] J.-M. Poumirol, A. Cresti, S. Roche, W. Escoffier, M. Goiran, X. Wang, X. Li, H. Dai, and B. Raquet, Phys. Rev. B **82**, 041413(R) (2010).
[28] J. C. Meyer, A. K. Geim, M. I. Katsnelson, K. S. Novoselov, T. J. Booth, and S. Roth, Nature (London) **446**, 60 (2007).
[29] T. Kawarabayashi, Y. Hatsugai, and H. Aoki, Phys. Rev. Lett. **103**, 156804 (2009).
[30] W. Zhu, Q. W. Shi, J. G. Hou, and X. R. Wang, e-print arXiv:1006.0545v1.
[31] A. Fasolino, J. H. Los, and M. I. Katsnelson, Nat. Mater. **6**, 858 (2007).
[32] J. W. Klos, A. A. Shylau, I. V. Zozoulenko, Hengyi Xu, and T. Heinzel, Phys. Rev. B **80**, 245432 (2009).
[33] Z. Qiao, S. A. Yang, W. Feng, W.-K. Tse, J. Ding, Y. Yao, J. Wang, and Q. Niu, Phys. Rev. B **82**, 161414(R) (2010).